

An Arabidopsis berberine bridge enzyme-like protein specifically oxidizes cellulose oligomers and plays a role in immunity[†]

Federica Locci¹, Manuel Benedetti^{1,‡}, Daniela Pontiggia¹, Matteo Citterico¹, Claudio Caprari², Benedetta Mattei³ , Felice Cervone¹ and Giulia De Lorenzo^{1,*}

¹Dipartimento di Biologia e Biotechnologie 'Charles Darwin', Sapienza Università di Roma, Piazzale Aldo Moro 5, 00185, Rome, Italy,

²Dipartimento di Bioscienze e Territorio, Università degli Studi del Molise, Contrada Fonte Lappone I-86090, Pesche (IS), Italy, and

³Dipartimento MESVA, Università dell'Aquila, Piazzale Salvatore Tommasi 1, 67100 Coppito (AQ), Italy

Received 2 October 2018; revised 5 January 2019; accepted 11 January 2019; published online 21 January 2019.

*For correspondence (e-mail giulia.delorenzo@uniroma1.it).

[†]Dedicated to the memory of Jonathan D. Walton.

[‡]Present address: Dipartimento di Biotechnologie, Università di Verona, Verona, Italy.

SUMMARY

The plant cell wall is the barrier that pathogens must overcome to cause a disease, and to this end they secrete enzymes that degrade the various cell wall components. Due to the complexity of these components, several types of oligosaccharide fragments may be released during pathogenesis and some of these can act as damage-associated molecular patterns (DAMPs). Well-known DAMPs are the oligogalacturonides (OGs) released upon degradation of homogalacturonan and the products of cellulose breakdown, i.e. the cellodextrins (CDs). We have previously reported that four Arabidopsis berberine bridge enzyme-like (BBE-like) proteins (OGOX1–4) oxidize OGs and impair their elicitor activity. We show here that another Arabidopsis BBE-like protein, which is expressed coordinately with OGOX1 during immunity, specifically oxidizes CDs with a preference for cellotriase (CD3) and longer fragments (CD4–CD6). Oxidized CDs show a negligible elicitor activity and are less easily utilized as a carbon source by the fungus *Botrytis cinerea*. The enzyme, named CELLOX (cellodextrin oxidase), is encoded by the gene *At4 g20860*. Plants overexpressing CELLOX display an enhanced resistance to *B. cinerea*, probably because oxidized CDs are a less valuable carbon source. Thus, the capacity to oxidize and impair the biological activity of cell wall-derived oligosaccharides seems to be a general trait of the family of BBE-like proteins, which may serve to homeostatically control the level of DAMPs to prevent their hyperaccumulation.

Keywords: cellodextrins, damage-associated molecular patterns, DAMPs, *Botrytis cinerea*, cell wall-derived oligosaccharides, *Arabidopsis thaliana*.

INTRODUCTION

The plant cell wall contains a complex mixture of polysaccharides that represent a physical barrier to pathogenic microbes (Ferrari *et al.*, 2013; Malinovsky *et al.*, 2014; Lampugnani *et al.*, 2018). To overcome this barrier, pathogenic microbes secrete cell wall-degrading enzymes (CWDEs) such as polygalacturonases (PGs), hemicellulases and cellulases, which target different cell wall components. Cell wall-degrading enzymes are produced sequentially during infection, and as well as causing the necessary breaches in the cell wall to allow microbial invasion they may release oligosaccharides that, upon recognition by specific plant receptors, trigger plant immunity. These cell wall

fragments therefore behave as damage-associated molecular patterns (DAMPs) (Boutrot and Zipfel, 2017; Gust *et al.*, 2017). In addition, endogenous plant-derived CWDEs, which participate in the dynamics and remodeling of the cell wall during growth and development or are induced during mechanical rupture of the cell wall (Tucker *et al.*, 2018), may potentially release cell wall fragments with regulatory and elicitor activity. These may be perceived as signals in the context of a cell wall integrity sensing system devoted to monitoring cell wall status and the correct coordination of biochemical and mechanical cues (Savatin *et al.*, 2014b; Wolf, 2017; De Lorenzo *et al.*, 2018a,b; Engelsdorf *et al.*, 2018; Franck *et al.*, 2018).

Considering the complexity of the plant cell wall, many types of fragments can theoretically be released either by pathogen-derived enzymes during an attempted invasion or by endogenous enzymes during physiological rupture/remodeling of the cell wall. Oligogalacturonides (OGs), derived from the degradation of homogalacturonan, are well-known DAMPs but also behave as molecules that regulate growth and development (Ferrari *et al.*, 2013; Cervone *et al.*, 2015). Besides OGs, the degradation products of cellulose, i.e. cellodextrins (CDs), have been shown to act as DAMPs in both grapevine (Aziz *et al.*, 2007) and Arabidopsis (Souza *et al.*, 2017) and, very recently, the hemi-cellulose-derived xyloglucan has also been reported to act as a DAMP in grapevine and Arabidopsis (Claverie *et al.*, 2018). In Arabidopsis, cellobiose (CD2) has been reported to be very active in triggering a signaling cascade similar to that triggered by OGs but it is unable to induce the production of reactive oxygen species (ROS) or callose deposition (Souza *et al.*, 2017). On the other hand, celotriose (CD3) induces cytoplasmic calcium elevation, changes in membrane potential, production of ROS and expression of genes involved in defense, such as those encoding the NADPH oxidase RBOHD, the mitogen-activated protein kinase MPK3, the key regulator of salicylic-mediated signaling NPR1 and the lipoxygenase LOX1, as well as genes involved in growth and root development (Johnson *et al.*, 2018). Indeed, CD3 produced by *Piriformospora indica*, an endophytic root-colonizing fungus, has been shown to play a role in interaction with Arabidopsis by promoting plant growth and inducing resistance against biotic and abiotic stresses (Johnson *et al.*, 2018).

Damage-associated molecular patterns may act as important signals in the so-called growth–defense trade-off, namely reduced plant growth as a consequence of metabolic diversion towards defenses (Huot *et al.*, 2014). Activation of the immune system also poses the risk of an exaggerated response that may be deleterious rather than advantageous and, if the immune response persists beyond the necessary time, it may lead to hyper-immunity characterized by an excessive reduction of growth and, in some cases, cell death. For example, an intense release of OGs leads to reduced growth (Benedetti *et al.*, 2015) and may even cause cell death (Cervone *et al.*, 1987; Benedetti *et al.*, 2015). Therefore, it is conceivable that the response to these signals is subject to strict control through homeostatic mechanisms aimed at the prevention of hyper-immunity.

A mechanism that is likely to regulate the homeostasis of OGs has recently been discovered in Arabidopsis. This relies on the activity of four berberine bridge enzyme-like (BBE-like) proteins, named *OGOX1* [At4g20830 or *BBE20* according to the nomenclature reported in Daniel *et al.* (2015)], *OGOX2* (At4g20840/*BBE21*), *OGOX3* (At1g11770/*BBE2*) and *OGOX4* (At1g01980/*BBE1*) (Benedetti *et al.*,

2018). These enzymes have a FAD-binding domain, carry a N-terminal signal peptide for translocation into the endoplasmic reticulum (ER) and oxidize the galacturonic acid at the reducing end of OGs into galactaric acid, with the production of hydrogen peroxide (H₂O₂). Oxidized OGs display a much reduced ability to induce defense responses. Nevertheless overexpression of *OGOX1* confers increased resistance against *Botrytis cinerea* because the oxidation of OGs impairs their full utilization as a carbon source by the fungus (Benedetti *et al.*, 2018). The BBE-like enzymes that oxidize glucose and, to a minor extent, CD2, cellotetraose (CD4) and cellopentaose (CD5) have been described to behave as antifungal proteins in sunflower *Helianthus annuus* and *Lactuca sativa* (Custers *et al.*, 2004).

In this work, we identify an Arabidopsis member of the BBE-like protein family, At4g20860, as an enzyme capable of specifically oxidizing cellulose fragments but not glucose. We report here the biochemical characterization of the enzyme and show that the enzymatic oxidation of CDs reduces their elicitor activity. As in the case of oxidized OGs, the use of oxidized CDs as a carbon source does not allow the growth of *B. cinerea* and, as a consequence, overexpression of the CD-oxidizing enzyme *in planta* restricts plant colonization by the fungus. We suggest that oxidation of cell wall-derived oligosaccharides performed by BBE-like enzymes is an important function of this family dedicated to the homeostasis of DAMPs.

RESULTS

The expression of *At4g20860* and *OGOX1* is coordinated during immunity

Much of the function of the 27 members of the Arabidopsis BBE-like protein family (shown in the homology tree in Figure S1a in the online Supporting Information) is still unknown. Transgenic plants expressing the so-called OG-machine (OGM), a chimeric protein comprising the polygalacturonase-inhibiting protein 2 from *Phaseolus vulgaris* and the PG from *Fusarium phyllophilum* under a β -estradiol-inducible promoter, were instrumental for the identification of four BBE-like proteins as specific oxidases of OGs (Benedetti *et al.*, 2018). Because enzymes that possess activity towards oligosaccharides other than OGs have never been identified in Arabidopsis, we used the plants expressing the OGM to search for possible oxidizing activity of a cell wall fragment that, like OGs, has been reported to act as a DAMP, the cellobiose (CD2) (Souza *et al.*, 2017). Total protein extracts from β -estradiol-induced plants expressing the OGM were assayed against CD2 and several saccharides including OGs. Oxidizing activity was found towards CD2 but not against the other sugars (Figure 1a). Chromatographic separation on a sulfopropyl Sepharose (SP Sepharose) cation exchange column of the protein extracts showed that the profile of the

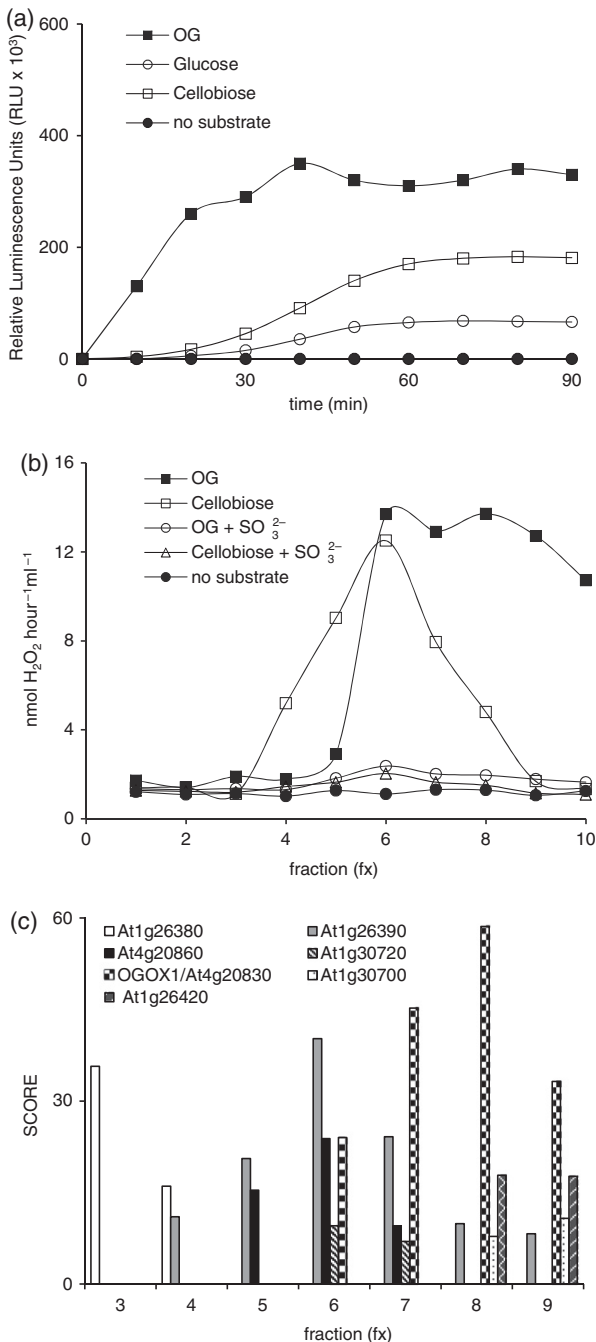


Figure 1. Carbohydrate-oxidizing activity and berberine bridge enzyme (BBE)-like proteins in β -estradiol-induced OG-machine (OGM) plants. (a) Activity of protein extracts, analyzed by measuring the production of H₂O₂ through a luminol peroxidase-based assay, after supplying the indicated carbohydrates as substrates to the reaction mixture. Fucose, rhamnose, xylose and galactose gave results similar to the 'no substrate' sample. OG, oligogalacturonide. (b) Activity in the fractions eluted from a sulfopropyl (SP) Sepharose column loaded with the protein extracts from the OGM plants, analyzed by supplying OGs and cellobiose to each fraction in the presence and in the absence of 1 mM SO₃²⁻ and measuring the H₂O₂ produced through an orange xylene-based assay. (c) Identification of BBE-like proteins in the fractions eluted from the SP Sepharose column as determined by LC-MS/MS analysis. Score indicates the sum of the ion scores of all peptides that were identified for each BBE-like enzyme.

CD2-oxidizing activity was sulfite-sensitive and differed from that of the OG-oxidizing activity (Figure 1b). Activity was mainly present in the fractions containing the proteins At4g20860/BBE22 and At1g26390/BBE4, identified by LC-MS/MS analysis (Figure 1c, Data S1). Other BBE-like proteins were identified by LC-MS/MS analysis in the fractions of SP Sepharose column chromatography. Fraction 3 displayed no CD2- or OG-oxidizing activity and contained the enzyme FOX1/RET-OX encoded by the gene *At1g26380/BBE3* that catalyzes the conversion of indole-3-acetaldoxime (IAOx) to indole-3-carbonyl nitrile, a metabolite with a role in defense (Rajniak *et al.*, 2015). The accumulation of the *At1g26380/BBE3/FOX1/RET-OX* transcripts has been widely used as a readout of the response to elicitors (Denoux *et al.*, 2008). Fraction 9 did not display CD2-oxidizing activity and contained the proteins At1g26420/BBE7, At1g30700/BBE8 and At1g26390/BBE4. The last protein is closely related to FOX1 (Figure S1a) and is unlikely to be an enzyme capable of oxidizing carbohydrates. Within the whole BBE-like family, the expression of the *At4g20860/BBE22* gene was very similar to that of *OGOX1/At4g20830* in response to several treatments representative of a biotic stress, as determined by hierarchical clustering analyses of the publicly available microarray data (Figures 2a and S2). We therefore assessed, by quantitative RT-PCR (qRT-PCR), whether *OGOX1* and *At4g20860* are similarly expressed in response to infection and elicitors. Leaves infected with *B. cinerea* showed expression of both genes at 16, 24 and 48 h post-infection (Figure 2b). Expression of both genes in seedlings was induced in response to flg22, elf18 and OGs. However, only *At4g20860* responded to CD3 while CD2 did not significantly induce either *OGOX1* or *At4g20860* (Figure 2c,d). We focused on *At4g20860* as a candidate gene encoding an oxidase of cellulose fragments.

The protein encoded by *At4g20860* is a cellodextrin oxidase (CELLOX)

For biochemical characterization, the *At4g20860* protein was expressed in *Pichia pastoris* as a secreted protein and tagged at the C-terminal with Myc-His epitopes. The presence of oxidizing activity in the medium of the recombinant *P. pastoris* towards OGs, xyloglucan, carboxy-methylcellulose (CMC), CD2 and several monosaccharides was tested by measuring the amount of H₂O₂ produced in the reaction mixture. As shown in Figures 3(a) and S3, activity was detected only by using CD2 as a substrate. The CD2-oxidizing activity was purified through two sequential ion exchange chromatography steps. The culture medium of *P. pastoris* was loaded on an anion exchange diethylaminoethyl-cellulose column and eluted with 1 M NaCl. Oxidizing activity was mainly detected in the flow-through (Figure S4a), which was then loaded on a cation exchange SP Sepharose column and subjected to stepwise elution

with increasing concentrations of NaCl (0.2, 0.5 and 1 M). Activity was recovered in the fraction eluted with 0.2 M NaCl (Figure S4a). The CD2-oxidizing activity was optimal at pH 6.8 (Figure 3b) and exhibited good thermal stability (Figure S4b). By using as substrates CDs with a degree of polymerization between 2 and 6 the calculated kinetic parameters indicated that the activity of the enzyme on longer oligomers is higher than on cellobiose. The calculated K_m is at least 40 times lower for CD3, CD4, CD5 and cellobiose (CD6) than for CD2 and a higher V_{max} was detected by using CD3 as a substrate (Figure 3c, Data S2). Overall, these data indicate that CD3 is the cellulose fragment that is more efficiently oxidized by the enzyme. Oxidation of CDs caused the conversion into gluconic acid of the glucose residue at the reducing end, as assessed by high-performance anion exchange chromatography with pulsed amperometric detection (HPAEC-PAD) and MS analyses (Figure S5 shows representative analyses of the oxidation of CD3 and CD4). Thereby, the enzyme encoded by *At4g20860* was named CELLOX (for cellodextrin oxidase).

The *CELLOX/At4g20860* gene is intron-less and clustered with *OGOX1*, *OGOX2* (*At4g20840*) and two other BBE-like genes of unknown function (*At4g20800* and *At4g20820*) in a single locus on chromosome 4 (Figure S6a). CELLOX is a putative apoplastic protein sharing a similarity of 78.88% with its only close paralog (*At5g44360*) and 55.58% with *OGOX1*. Similarity with the recently characterized cellobiose oxidase of *Physcomitrella patens* (here indicated as PpCBOX) is lower, at 40.77% (Toplak *et al.*, 2018). Homology analysis including PpCBOX and the true BBE enzyme P30986 from *Eschscholzia californica* (California poppy), which is involved in the formation of benzophenanthridine alkaloids and is the BBE family's namesake (Winkler *et al.*, 2006), supports the view that the diversification of plant BBEs and BBE-like paralogs occurred after the separation between mosses and higher plants, with the true BBE being evolutionarily the most recent (Toplak *et al.*, 2018).

Structural modeling of CELLOX showed the known features of BBE-like proteins (Daniel *et al.*, 2017): (i) the bivalent linkage of the FAD isoalloxazine ring via the C6- and 8 α -position to a cysteine and histidine residue (H91 and C154), respectively; (ii) the remarkable conservation of the overall fold, also with respect to PpCBOX, as already discussed by other authors (Daniel *et al.*, 2016; Toplak *et al.*, 2018); and (iii) the presence of a relatively large active site (Figures 4a and S7a,b). CELLOX carries a type IV active site (Figure S7c) (Daniel *et al.*, 2016) that, within the Arabidopsis BBE-like protein family, is shared only by its closest paralog *At5g44360/BBE23*. The representative structure for the type IV active site has been described in the grass pollen allergen Phl p 4, another BBE-like enzyme (Zafred *et al.*, 2015). As expected, the wide positively charged region that is present in *OGOX1* is absent in CELLOX, which shows a

denser distribution of negative charges around the active site compared with the other carbohydrate oxidases (Figure 4a). Amino acid sequence alignment shows several acidic residues that are specifically present in CELLOX and its closest paralog (Figure 4b) as well as H92 and C154 involved in the bivalent binding of FAD, the conservation of the oxygen gatekeeper valine (V157) and the surrounding residues (Figures 4b, S6b and S7a,b). Moreover, several aromatic amino acids are present within and in the proximity of the active site (Figure S7b,c), which may participate in substrate binding, as observed in the interaction of microbial expansins with CD6 (Cosgrove, 2017).

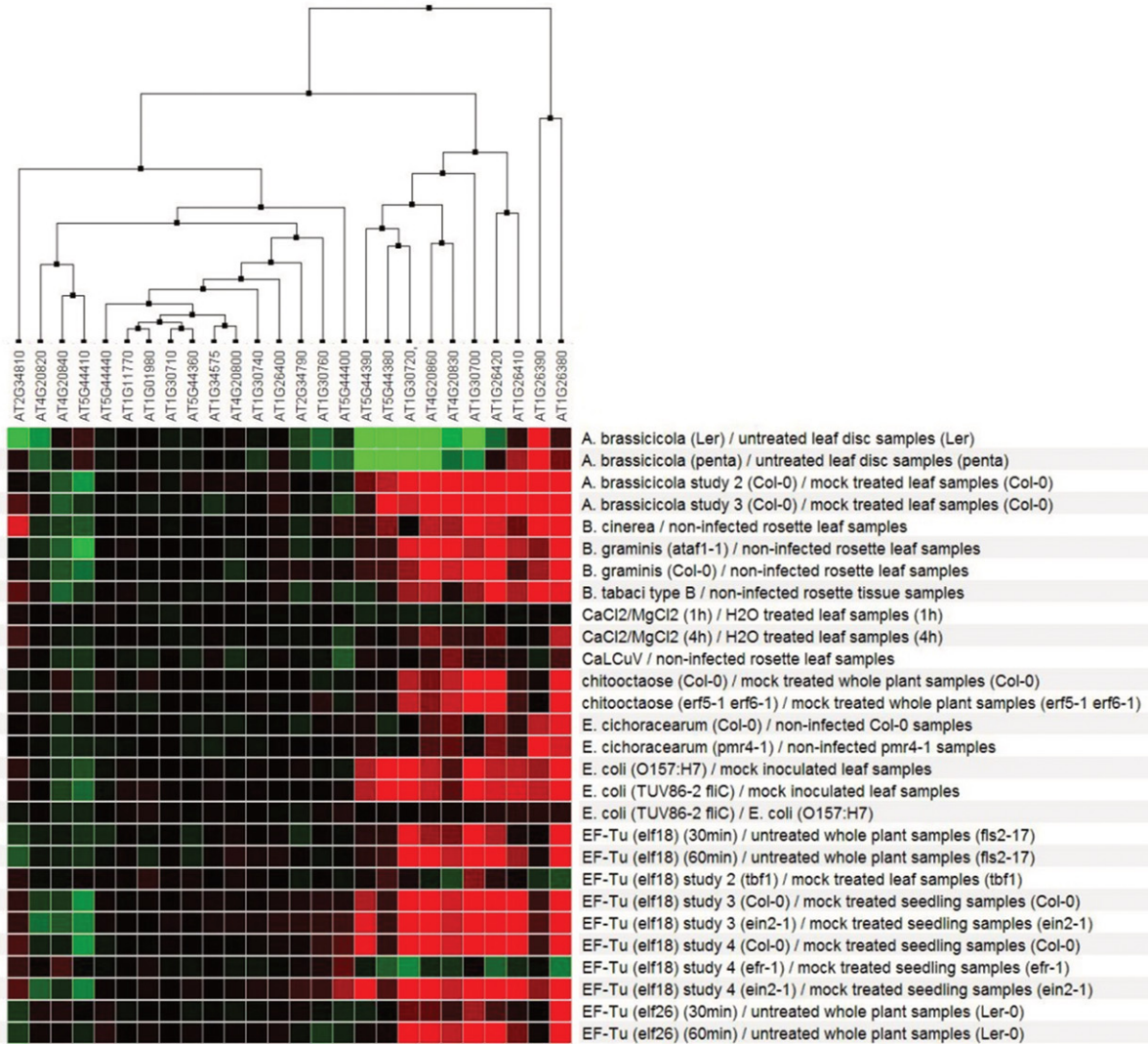
Oxidation impairs the elicitor activity of cellodextrins

The elicitor capability of CD2, CD3, CD4, CD5 and CD6 was investigated using Arabidopsis Columbia-0 (Col-0) seedlings. Early induced immune responses were analyzed, including the expression of *RBOHD* and *WRKY30* as readouts of CD action (Souza *et al.*, 2017; Johnson *et al.*, 2018), and of *CYP81F2* as a readout of OG action (Savatin *et al.*, 2014a; Gravino *et al.*, 2015), as well as phosphorylation of the mitogen-activated protein kinases (MAPKs) MPK3/MPK6 and ROS production. All CDs tested, with the exception of CD2, were able to induce the expression of the defense genes examined (Figure 5a), MAPK phosphorylation (Figure 5b) and ROS production (Figure 5c). The highest activity was shown by CD3, comparable to that of OGs (Figure 5a–c). However, maximal production of ROS with CDs was observed after 18 min, i.e. about 10 min later than with OGs (Figure 5c). Next, the effect of the oxidation on CD elicitor activity was investigated. Oxidized CD3 and CD4 were prepared using CELLOX purified from *P. pastoris* and their purity was assessed by HPAEC-PAD and MS analyses (Figure S5). The oxidized oligosaccharides displayed very limited or no capability of inducing the early expression of *RBOHD*, *WRKY30* and *CYP81F2* (Figure 5d), thereby showing that oxidation of CDs by CELLOX impairs their elicitor activity.

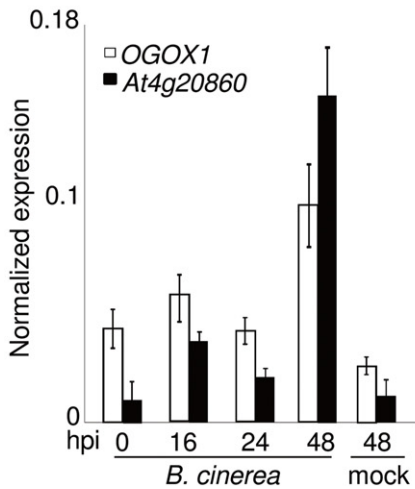
Overexpression of CELLOX indicates a role in immunity

The effect of high levels of CELLOX on the response to pathogens was explored. Five independent homozygous single-insertion T₃ lines overexpressing *CELLOX* were generated (*CELLOX*-OE #2.6, #4.4, #7.2, #8.5 and #9.7). Transcript levels of the transgene (Figure 6a) and enzymatic activity against CD3 (Figure 6b) were measured in adult leaves of the transgenic plants. Line 9.7 showed the highest expression of both transcript level and enzyme activity. Overexpressing lines 9.7 and 7.2 were chosen for further analyses; line 4.4, which showed *CELLOX* transcripts and enzyme activity similar to the wild type, was included as a control. Infection assays were performed using the necrotrophic fungus *B. cinerea*. The infected leaves of lines 9.7 and 7.2, but not those of the control line 4.4, showed

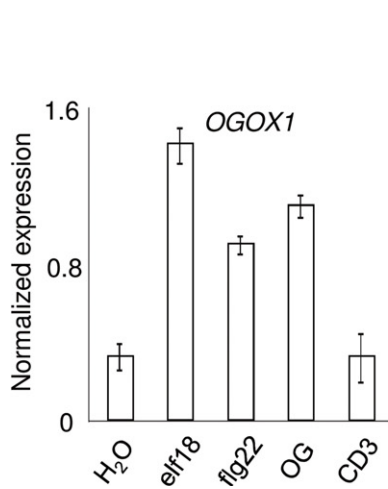
(a)



(b)



(c)



(d)

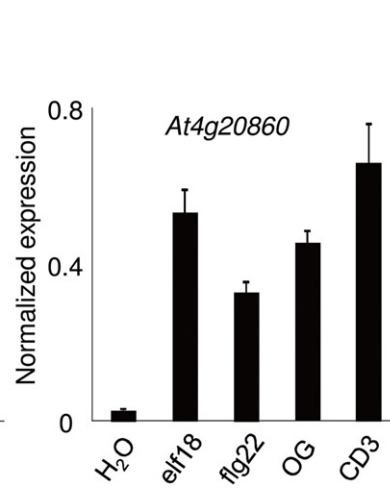


Figure 2. Expression of both *At4g20860* and *OGOX1* is upregulated upon infection with *Botrytis cinerea* and elicitation with elf18, flg22 and oligogalacturonides (OGs). Only the expression of *At4g20860* is upregulated by cellotriose (CD3). (a) Representative heatmap of expression of the 27 members of the berberine bridge enzyme (BBE)-like gene family during pathogen infection or elicitor treatment. The red and green colors indicate induction and repression, respectively. The hierarchical clustering generated from publicly available microarray data using Genevestigator (Hruz *et al.*, 2008) is shown at the top. The complete heatmap obtained from the analysis is shown in Figure S2. (b) Adult leaves were drop-inoculated with 5×10^5 *Botrytis cinerea* conidia or mock (potato dextrose broth). Transcript levels of *At4g20860* and *OGOX1* were analyzed by quantitative RT-PCR at the indicated times (hours post-inoculation, hpi). (c), (d) Seedlings were treated with elf18 (10 nM), flg22 (10 nM), OGs (25 $\mu\text{g ml}^{-1}$) or CD3 (25 $\mu\text{g ml}^{-1}$) for 30 min and *OGOX1* and *At4g20860* transcript levels were analyzed by quantitative RT-PCR and normalized to *UBQ5* expression.

smaller lesions than in the wild type (Figure 6c), indicating that the presence of high levels of the enzyme restricts the fungal infection. We have previously shown that oxidation of OGs decreases their value as a carbon source for *B. cinerea*, making plants that overexpress *OGOX1* more resistant to the fungus (Benedetti *et al.*, 2018). We therefore assessed whether oxidized CDs are also a less valuable carbon source for *B. cinerea*. The fungus was grown in a minimal medium to which non-oxidized CD3 (positive control) or purified oxidized CD3 was added, as a sole carbon source. After 7 days of culture, growth of the fungus was observed in the presence of CD3 but not of oxidized CD3 (ox-CD3) (Figure 6d). Moreover, *B. cinerea* grown on a medium supplied with both CD3 and ox-CD3 showed fungal growth very similar to that of the fungus in the medium supplied only with CD3. These data indicate that oxidized CD3 cannot be utilized by the fungus as a carbon source but does not act as an antimicrobial compound.

CELLOX-overexpressing plants oxidize CD3 more efficiently than wild-type plants

The presence and the levels of oxidized CD3 were investigated in leaves of wild-type and CELLOX-overexpressing plants, upon syringe-infiltration of water or CD3, and HPAEC-PAD analysis of the intercellular washing fluids (IWFs) prepared 30 min after the infiltration. The chromatographic profiles of the IWFs from wild-type and transgenic plants were similar upon infiltration of water (Figure 7a,b). Upon infiltration of CD3 a predominant peak corresponding to the non-oxidized CD3 was observed in the wild-type plants while a peak corresponding to the oxidized CD3 was mainly detected in the CELLOX-overexpressing plants (Figure 7c,d). This result clearly demonstrates that CELLOX is active *in planta* and rapidly oxidizes the infiltrated CD3.

DISCUSSION

Previous reports show that CDs behave as DAMPs in grapevine and Arabidopsis (Aziz *et al.*, 2007; Souza *et al.*, 2017). In our analyses the defense genes *RBOHD*, *WRKY30* and *CYP81F2* were strongly induced by CD3 and, to a lesser extent, by CD4, CD5 and CD6, while the elicitor activity of CD2 was negligible. In this work, we have identified a cellodextrin oxidase named CELLOX encoded by *At4g20860* that oxidizes and inactivates CDs, with a preference for CD3. Thus, in addition to enzymes that oxidize

OGs, the Arabidopsis family of BBE-like proteins is shown here to contain one more enzyme that oxidizes cell wall-derived DAMPs. Our observations confirm that the BBE-like family, in addition to other functions, may have the important role of maintaining the homeostasis of cell wall-derived DAMPs and regulating their activity. The genes encoding CELLOX, *OGOX1* and *OGOX2* are located in the same locus, although CELLOX does not exhibit a high similarity to the *OGOXs* (Benedetti *et al.*, 2018). It is likely that during evolution both diversification and duplication have shaped this locus for defense functions. The presence of both *OGOXs* and CELLOX in a single locus may respond to the need to coordinate the regulation of both types of enzymes either at the promoter or at the chromatin level. Indeed, CELLOX and *OGOX1* show a remarkably similar expression profile during immunity, suggesting that their activity is coordinated. The hierarchical clustering analysis of the expression profiles of the whole BBE-like gene family, beside the small clade comprising *At4g20860* and *OGOX1*, showed a second immunity-related clade comprising the five other BBE-like genes whose products were among the proteins identified in Figure 1(c), plus three other members of the family (see Figures 2a and S1a). Thus, at least 10 BBE-like members are likely to play a role in immunity.

CELLOX does not show a high similarity to previously described carbohydrate oxidases such as HaCHOX and LsCHOX (see Figure S1). HaCHOX prefers glucose as a substrate and shows decreasing activity on CDs of increasing size (Custers *et al.*, 2004). CELLOX does not oxidize glucose and has a preference for CDs with a degree of polymerization higher than 2, especially CD3. CELLOX is the only BBE-like enzyme so far identified that oxidizes cellulose fragments but not glucose and it is different from Nectarin V of tobacco, which is a glucose oxidase (Carter and Thornburg, 2004). PpCBOX, which oxidizes CD2 and lactose but not glucose, appears to be more similar to CELLOX; this enzyme, however, does not oxidize CD3 (Toplak *et al.*, 2018). Notably, CELLOX carries a type IV active site (Huang *et al.*, 2005), similar to the gluco-oligosaccharide oxidase from the saprophytic fungus *Sarocladium strictum* (Vuong *et al.*, 2013). The type IV active site is found in BBE-like proteins from fungi and lower plants (Daniel *et al.*, 2017). The affinities of CELLOX and the fungal enzyme for

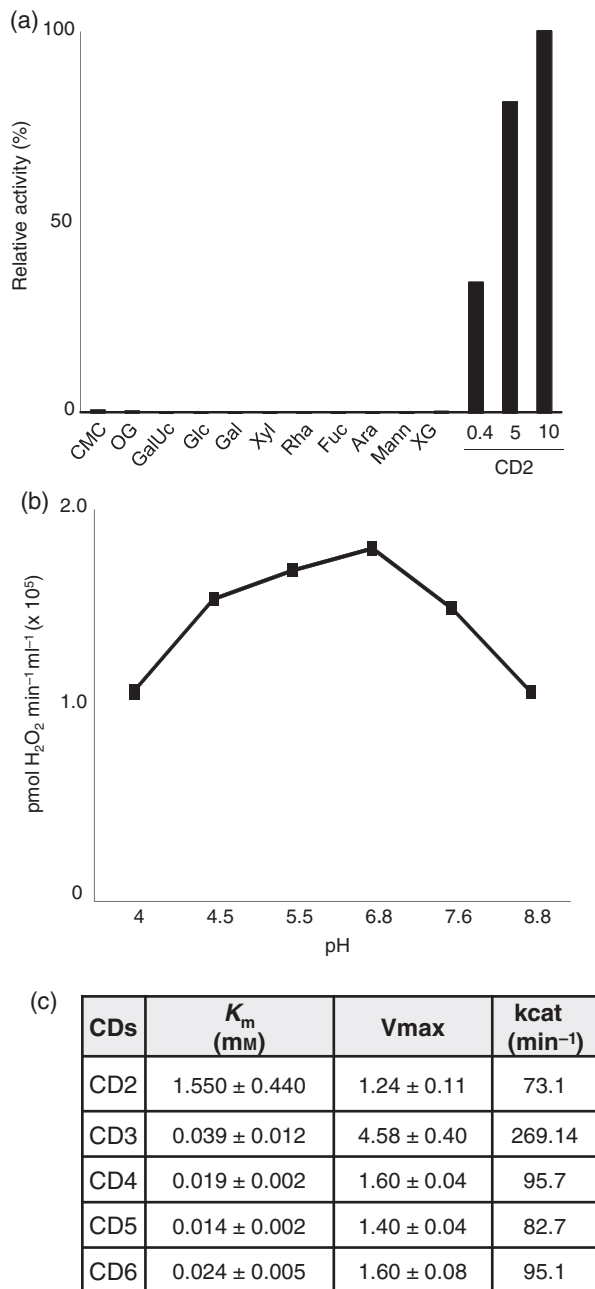


Figure 3. Substrate specificity and biochemical features of cellobiose oxidase CELLOX. *Pichia pastoris* medium containing the recombinant CELLOX was tested for substrate specificity. Thirty microliters was added to the reaction buffer (50 mM TRIS-HCl, pH 7.6, 50 mM NaCl) containing the substrate. The reaction was performed at 30°C for 30 min. The H₂O₂ produced was measured using an orange xylenol colorimetric assay (OD₅₆₀). (a) Relative activity towards different types of sugars at a concentration of 0.4 mM except for cellobiose (CD2), which was used at 0.4, 5 and 10 mM. CMC, carboxy-methyl-cellulose; OG, oligogalacturonide; GalUc, glucuronic acid; Glc, glucose; Gal, galactose; Xyl, xylose; Rha, rhamnose; Fuc, fucose; Ara, arabinose; Mann, mannose; XG, xyloglucan. (b) The pH optimum analysis, performed at 30°C using CD2 (5 mM) as a substrate. (c) Calculated K_m , V_{max} and k_{cat} using CD2, cellotriose (CD3), cellotetraose (CD4), cellopentaose (CD5) and cellobiose (CD6) as substrates (see Data S2). V_{max} is expressed in $\mu\text{mol H}_2\text{O}_2 \text{ min}^{-1} \text{ mg}^{-1}$ enzyme. In (b) and (c), assays were performed using CELLOX partially purified from *Pichia* medium (sulfopropyl eluate).

CD3–CD6 are comparable, but in general the latter has a higher turnover with these CDs.

In our experiments, CD3 induces the defense genes *RBOHD*, *WRKY30* and *CYP81F2*, MAPK phosphorylation and the production of ROS, showing an elicitor activity similar to that of OGs and stronger than that of longer CDs. In our experiments, we observed a different timing of ROS production in response to CD3 and OGs that was not observed in previous experiments performed on grapevine suspension cultured cells (Aziz *et al.*, 2007). This difference is unlikely to be due to a faster diffusion of OGs into the tissues compared with CDs, since both molecules were vacuum infiltrated into the leaf disk for the bioassay. The observed difference may probably reflect different features of the early perception/transduction events of the two types of DAMPs. Moreover, CD3 emerges as both the best substrate for CELLOX and the best elicitor among the CDs used in our analyses, strongly pointing to a role for CELLOX, along with OGOXs, as components of an enzymatic system involved in the control and homeostasis of cell wall-derived DAMPs. The elucidation of such a role, however, is complicated by the redundancy of these enzymes. While we uncovered that there are at least four OGOXs (Benedetti *et al.*, 2018) and one CELLOX in Arabidopsis, it is not yet known how many CELLOXs exist. Double and multiple mutants are probably necessary to address their biological role. On the other hand, notwithstanding the reduced elicitor activity of oxidized CDs and oxidized OGs, overexpression of CELLOX and OGOX1 enhances the resistance to *B. cinerea* (Benedetti *et al.*, 2018). The enhanced resistance may depend at least in part on the difficulty that the fungus has in utilizing oxidized oligosaccharides as a carbon source, and we show that *in planta* the overexpressed CELLOX is functional and rapidly transforms CD3 into oxidized CD3. In addition, in plants overexpressing CELLOX and OGOXs, the production of H₂O₂ may contribute to making the plant immunity response more efficient. CELLOX and OGOXs therefore display an indirect antimicrobial activity against *B. cinerea* that is likely to cooperate with and support the antimicrobial activity of the plant CWDE-inhibiting proteins. The CWDE-inhibiting proteins and carbohydrate oxidases may synergistically act in plant defense. However, while the inhibitors require specific molecular recognition of microbial proteins that may possibly be evaded by pathogens (Casasoli *et al.*, 2009; Benedetti *et al.*, 2011, 2013), the activity of OGOXs and CELLOX does not.

Since the release of DAMPs without proper control poses the risk of activating an exaggerated response that may be deleterious to plant growth and survival, BBE-like proteins are good candidates for reducing the effects of the hyperaccumulation of DAMPs (De Lorenzo *et al.*, 2018b). Their redundancy suggests a need for a fine regulation at the level of both enzyme activity and

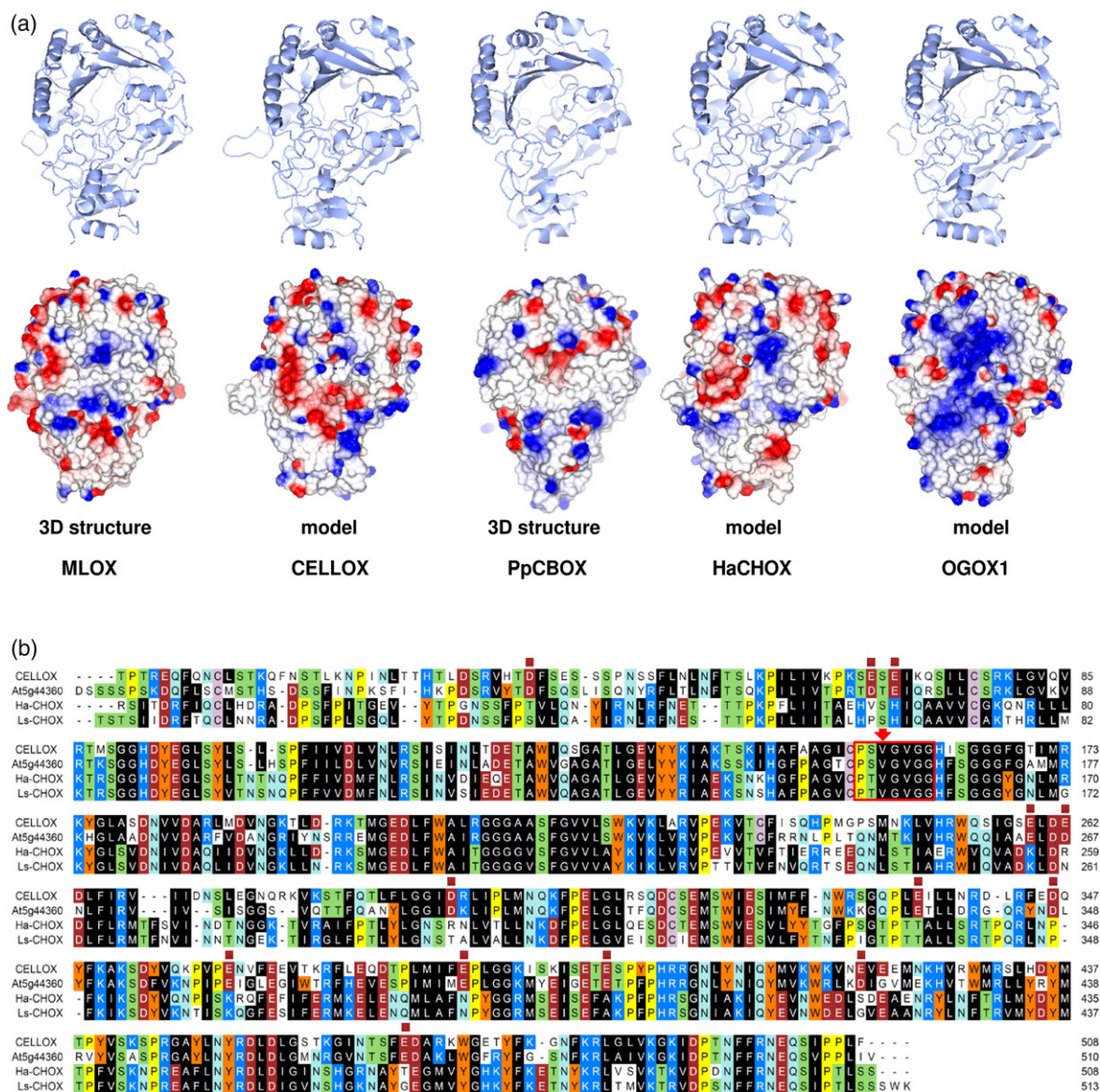


Figure 4. Shared and distinctive features of cellodextrin oxidase (CELLOX) and other berberine bridge enzyme (BBE)-like enzymes. (a) Electrostatic surface representation of CELLOX, *Helianthus annuus* carbohydrate oxidase (HaCHOX) and OGOX1, short isoform, all obtained by homology-based molecular modeling using as a template the crystallographic structure of the monoglucosyl oxidase At2g34790/BBE15 from *Arabidopsis thaliana*, shown on the left MLOX; code 4UD8 in the Protein Data Bank, <http://www.pdb.org>, and *Physcomitrella patens* cellobiose oxidase (PpCBOX). Red and blue indicate regions of negative and positive electrostatic potential, respectively. (b) Multiple amino acid alignment between the mature CELLOX, its closest paralog At5g44360, HaCHOX and *Lactuca sativa* carbohydrate oxidase (LaCHOX). Different colors highlight amino acids with different chemical properties; non-polar amino acids are shown in black. A red frame indicates the reactive oxygen motif (PTVGVGG) and the red arrow shows residue V157 of CELLOX as the oxygen reactivity gatekeeper residue. Black squares above the amino acid sequence indicate the sites involved in the covalent binding of the FAD cofactor; red squares indicate negatively charged residues at apoplastic pH that appear only in CELLOX and At5g44369. Numbering is from the first amino acid of the mature proteins.

transcription to ensure both robustness and tunability of the system. A more complete biochemical characterization of the BBE-like family may uncover how the activity of these enzymes may be finely regulated by the extracellular environment. For example, our data show that enzyme activity of both CELLOX (this work) and OGOXs (Benedetti *et al.*, 2018) is dependent on pH, and is higher at pH values higher than those occurring in the physiological

conditions of the apoplast. The alkalization that is typically induced by most elicitors may therefore lead to their activation. Moreover, in the case of OGOXs, different isoforms show a different pH dependence, pointing to a different regulation of the activity of these enzymes. The flavin cofactor itself may contribute to the regulation of the function of these enzymes, through its ability to function as a redox sensor (Becker *et al.*, 2012). Whether the

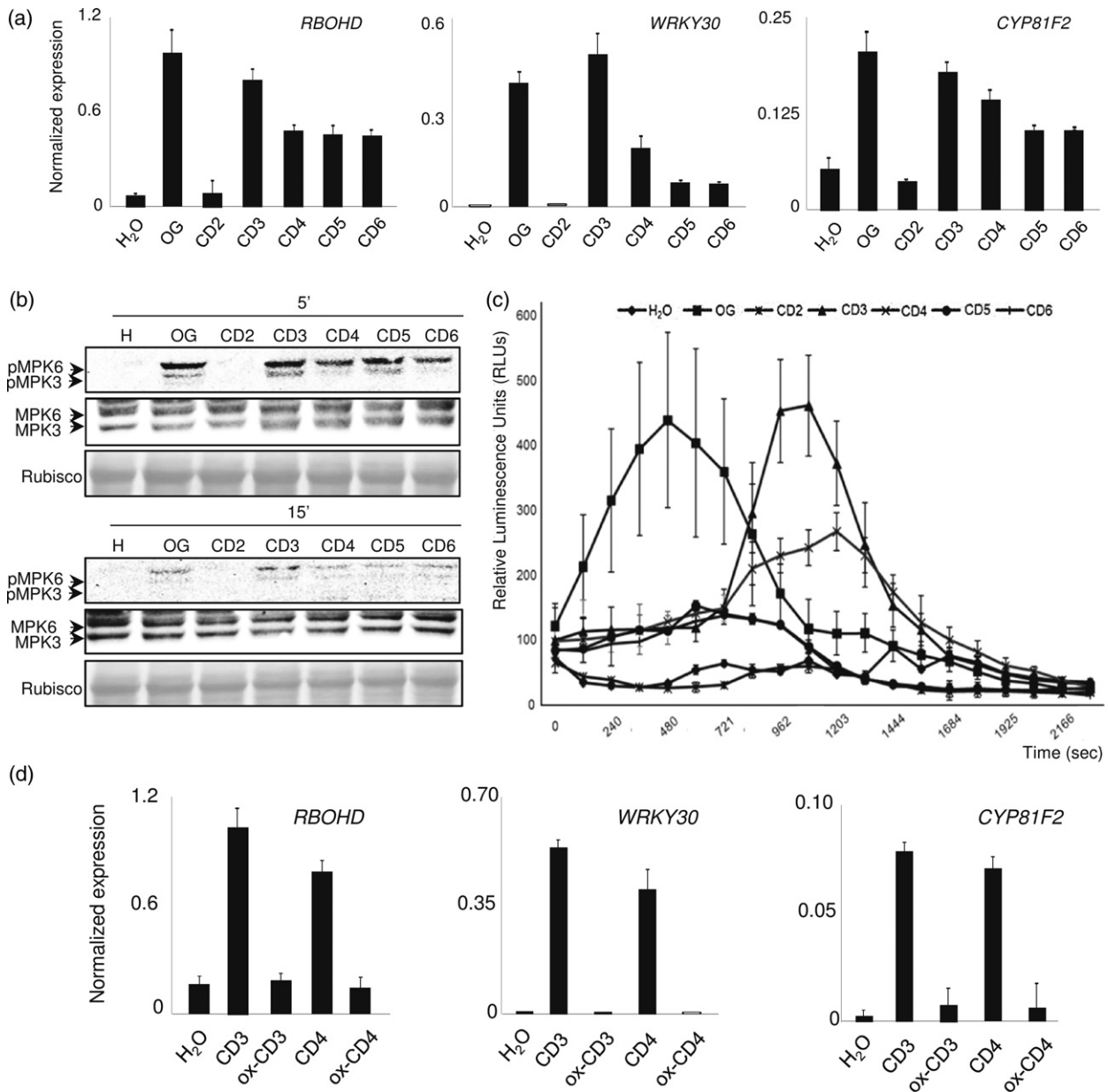


Figure 5. Cellohextrins (CDs) 3–6 are able to induce defense-related responses, whereas oxidized CDs are not. (a) Col-0 wild-type seedlings were treated for 30 min with $25 \mu\text{g ml}^{-1}$ of cellobiose (CD2), cellotriose (CD3), cellotetraose (CD4), cellopentaose (CD5), celloseaose (CD6), oligogalacturonides (OGs) or water (control). Transcript levels were analyzed by quantitative RT-PCR and normalized to *UBQ5* expression. (b) Levels of phosphorylated mitogen-activated protein kinases (MAPKs) MPK3 and MPK6 (pMPK3 and pMPK6) in seedlings of the wild-type (Col-0) after elicitation with OGs ($30 \mu\text{g ml}^{-1}$), CD2, CD3, CD4, CD5, CD6 ($30 \mu\text{M}$) or water (control) at the indicated time points were determined by immunoblot analysis using an anti-p44/42-ERK antibody (top panels). Levels of MPK3 and MPK6 total proteins were determined using specific antibodies (middle panels). Total proteins were detected by Ponceau Red staining and the Rubisco band is shown (bottom panels). The identity of individual MAPKs, as determined by their mobility, is indicated by arrows. (c) Production of H_2O_2 in 4-week-old leaves of Col-0 after treatment with OGs and CDs ($350 \mu\text{g ml}^{-1}$) was analyzed by a luminol/peroxidase-based assay. (d) Seedlings were treated for 30 min with $25 \mu\text{g ml}^{-1}$ of pure CD3, CD4 or pure oxidized CD3 and CD4 (ox-CD3 and ox-CD4) or water (control). Transcript levels were analyzed by quantitative RT-PCR and normalized to *UBQ5* expression.

important changes in the redox state of the apoplast occurring during the immune response modulate the activity of BBE-like proteins, by regulating the flavin redox state or the thiol/disulfide balance, which is also crucial for the regulation of the activity (Yi and Khosla, 2016;

Meyer *et al.*, 2019) is a key aspect to be investigated. On the other hand, elicitation and pathogen infection upregulate the expression of both OGOXs and CELLOX. Our data show that expression of CELLOX and OGOX1 is subject to different but also overlapping regulatory feedback loops,

Figure 6. Over-expression of cellodextrin oxidase (CELLOX) in transgenic *Arabidopsis* leads to enhanced basal resistance to *Botrytis cinerea*, which is not able to grow on oxidized cellotriose (ox-CD3) *in vitro*. Levels of (a) CELLOX transcripts and (b) CD3-oxidizing activity in adult leaves of plants overexpressing CELLOX (lines #2.6, #4.4, #7.2, #8.5 and #9.7). (c) Adult leaves of the wild type (Col-0) and CELLOX-OE (lines #4.4, #9.7 and #7.2) were drop-inoculated with *B. cinerea* conidia (5×10^5 conidia ml^{-1}). Lesion areas were measured at 48 h post-inoculation using ImageJ software. Bars indicate lesion areas (average \pm SE of at least three independent experiments; $n = 20$ lesions in each experiment). Asterisks indicate statistically significant differences compared to the control (Col-0), according to Student's *t*-test ($***P < 0.001$; $*P < 0.01$). (d) Dried *B. cinerea* mycelium biomass was measured after 7 days of growth in a medium supplemented with 0.15% CD3, purified ox-CD3 or both (CD3 + ox-CD3) as the sole carbon source. Water was used as a control. Asterisks indicate statistically significant differences compared with the fungus grown on CD3, according to Student's *t*-test ($***P < 0.001$). (e) Representative pictures of *B. cinerea* hyphae grown for 4 days as described in (c).

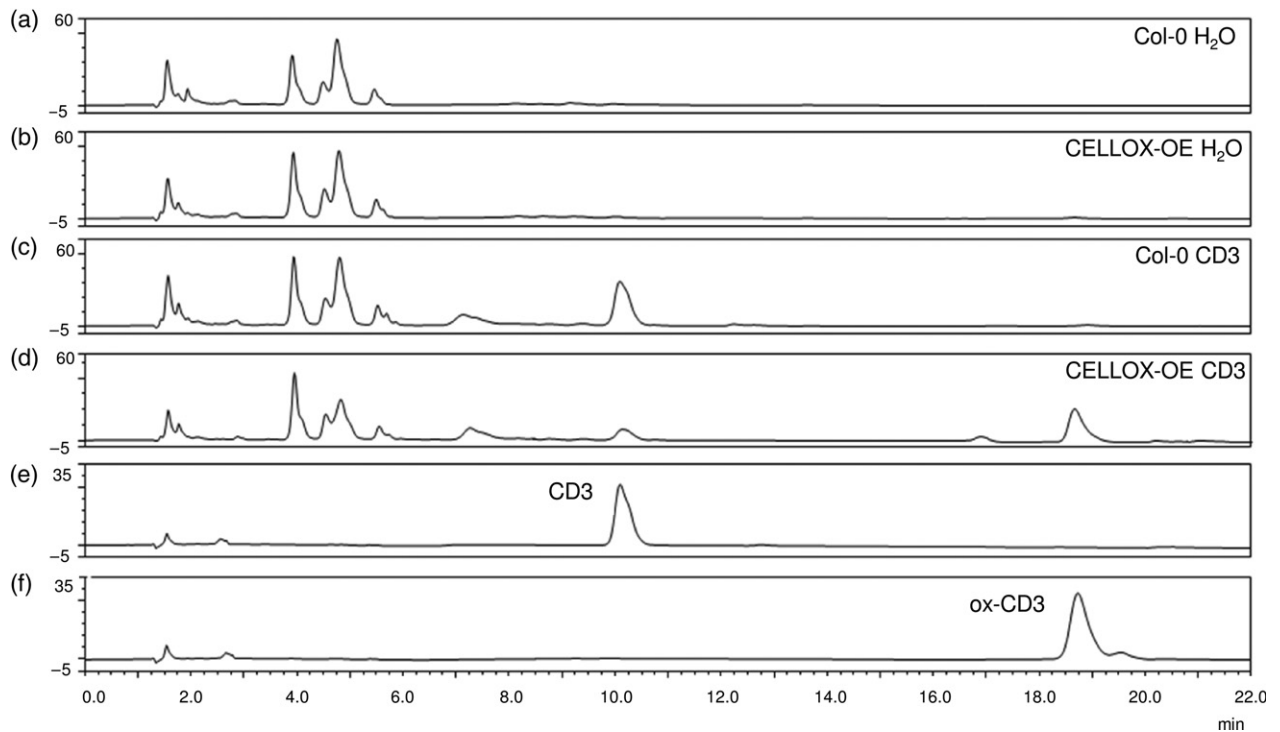
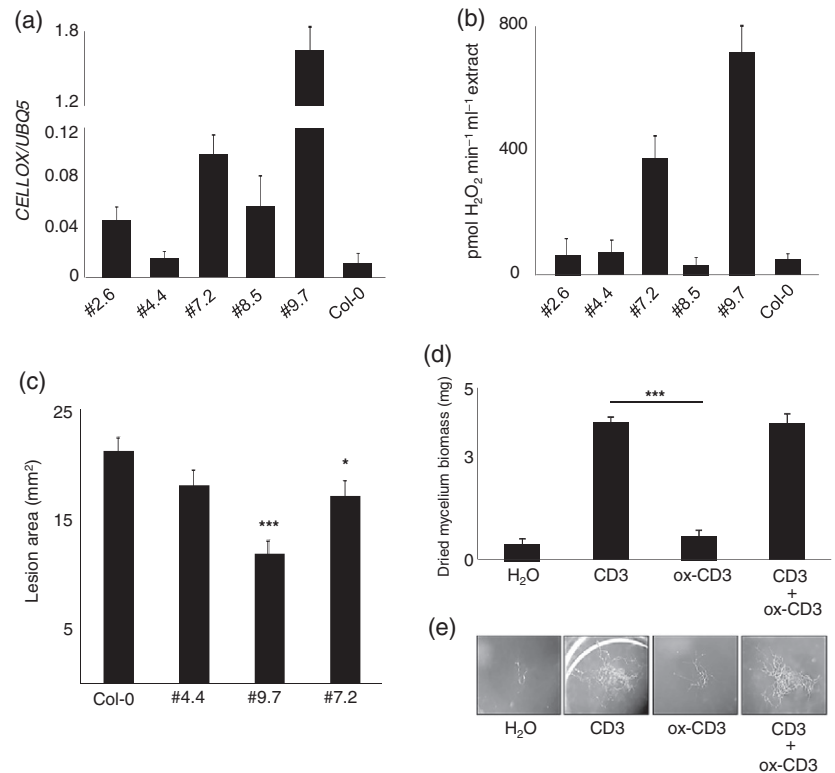


Figure 7. Enhanced oxidation of cellotriose (CD3) in cellodextrin oxidase (CELLOX)-overexpressing (OE) plants compared with wild-type plants. Chromatograms of intercellular washing fluids (IWFs) prepared from 4-week-old leaves of Col-0 (a) and CELLOX-OE plants (b) 30 min after infiltration with water. Chromatograms of IWF from Col-0 (c) and CELLOX-OE (d) leaves 30 min after infiltration with CD3. Chromatograms of pure CD3 (e) and oxidized CD3 (ox-CD3) (f). Graph shows signal intensity (nC) at each retention time (minutes).

since, for example, OGs and flg22 induce the expression of both enzymes whereas CD3 only induces the expression of *CELLOX*.

It can be speculated that other members of the BBE-like family may control the homeostasis of CW fragments other than OGs and CDs, probably constituting a battery of enzymes that are important for coping with alterations of cell wall integrity. The characterization of the BBE-like family, therefore, may potentially uncover novel cell wall bioactive fragments that are relevant in immunity and the growth–defense trade-off. The existence of cell wall-entrapped bioactive structures other than OGs has been hypothesized by several authors (Darvill *et al.*, 1994; Wolf, 2017; Bacete *et al.*, 2018; Engelsdorf *et al.*, 2018; Oelmüller, 2018) and recently the hemicellulose-derived xyloglucan has also been reported to act as a DAMP (Claverie *et al.*, 2018).

EXPERIMENTAL PROCEDURES

Plant material and growth

Arabidopsis (*Arabidopsis thaliana*) ecotype Col-0 wild-type seeds were purchased from Lehle Seeds (<http://www.arabidopsis.com/>). Seeds were washed twice in 1 ml of sterile water, then treated with 1 ml of sterilization solution (1.6% NaClO, 0.01% SDS) for 7 min in slow agitation, followed by seven washing steps in 1 ml of sterile water. For stratification, seeds were left in 50 μ l of sterile water for 4 days at 4°C. Col-0 seedlings were grown in liquid MS/2 medium [Murashige and Skoog medium including vitamins (2.2 g L⁻¹), 0.5% sucrose, pH 5.5] at 22°C and 70% relative humidity under a 16-h light/8-h dark cycle. Adult plants of Col-0 and *CELLOX*-OE were grown on soil at 22°C and 70% relative humidity under a 12-h light/12-h dark cycle (approximately 120 μ mol m⁻² sec⁻¹).

Enzyme assays

Carbohydrate-oxidizing activities were determined by measuring the H₂O₂ produced by the reaction using a luminol peroxidase-based assay (Roux *et al.*, 2011) or a xylenol orange colorimetric assay (Gay *et al.*, 1999), as indicated in the figure legends. Assays were performed at 30°C in 50 mM TRIS-HCl, 50 mM NaCl, at pH 7.8 for the identification of cellobiose-oxidizing activity in OGM plant extracts (Figure 1; for 12 h for Figure 1b), and at pH 6.8 for 30 min in all the other assays, unless otherwise indicated.

Identification of cellobiose-oxidizing activity

Total proteins were extracted from 5 g of fresh leaf material of OGM plants collected 170 h after spraying with 25 μ M β -estradiol using 20 ml of extraction buffer [20 mM Na-acetate pH 5.0, 0.8 M NaCl; ratio 4:1 (ml:g of tissue)]. Carbohydrate-oxidizing activities were determined by a luminol-based assay.

For enzyme separation, the protein extract was diluted 20-fold in 20 mM Na-acetate pH 5.0 and loaded on a 1 ml SP Sepharose FF column (GE Healthcare, <https://www.gehealthcare.com/>). Elution was carried out using a stepwise gradient of NaCl (from 0 to 1 M NaCl in 10 column volumes). Carbohydrate-oxidizing activity was evaluated in each eluted fraction by using standard OGs (1 mg ml⁻¹) or cellobiose (0.16 mg ml⁻¹) as substrates and the xylenol orange assay.

Protein digestion and proteomic analysis by LC-MS/MS

For each fraction obtained by protein extract of the OGM leaves after elution from the SP Sepharose cation exchange column, aliquots (100 μ l) were freeze-dried and dissolved in 100 μ l of freshly prepared 8 M urea in 10 mM TRIS-HCl pH 8.0. For each sample, proteins were subjected to reduction and alkylation of cysteines as previously described (Mattei *et al.*, 2016). Proteolytic digestion was carried out overnight with proteomics grade trypsin (Promega, <http://www.promega.com/>; trypsin:protein ratio 1:50) at 25°C. The digestion mixture was subsequently acidified with 1% (v/v) formic acid and centrifuged (10 000 g for 5 min) to remove insoluble material. Peptides were desalted using home-made microcolumns with R3 beads (Thermo Fisher, <https://www.thermofisher.com/>) packed in gel loader tips. Proteomic analysis by LC-MS/MS was performed as previously described (Benedetti *et al.*, 2018).

Expression of *CELLOX* in *Pichia pastoris* and its purification

The *At4g20860* DNA sequence encoding the mature form of *CELLOX* was amplified from *Arabidopsis* genomic DNA using the *EcoRI*-Fw and *NotI*-Rev primers (Table S1) and cloned in the *EcoRI*-*NotI* sites of the constitutive expression vector pGAPzA, downstream of the sequence encoding the yeast alpha factor signal peptide for translocation into the ER and upstream of the *c-myc*/*HIS* epitope-encoding sequence. The recombinant plasmid was introduced in *P. pastoris* by electroporation and transformants were grown in yeast extract (1%), peptone (2%) and glucose (2%) for 2 days. The culture was centrifuged (6000 g for 10 min) and the medium was collected and enzyme activity detected using 0.4 mM CD2 as a substrate.

Purification of *CELLOX* was performed by two sequential ion exchange chromatography steps. *Pichia* medium (20 ml) was loaded on a diethylaminoethyl-cellulose (DEAE) (Sigma-Aldrich) column (10 ml), previously washed with one column volume (CV) of high-salt buffer (1 M NaCl in 50 mM Na-acetate, pH 5.0) and then equilibrated with 5 CV of low-salt buffer (50 mM Na-acetate pH 5.0). Before loading, the pH of the *Pichia* medium was checked; since it was lower than 5.0, 3 M Na-acetate was added to obtain a final pH of 5.0. Flow-through was collected and adsorbed proteins were eluted with 1.5 ml of high-salt buffer. In the second chromatographic step, the flow-through of the DEAE column was loaded on an HiTrap SP-Sepharose FF (GE Healthcare) column (5 ml) previously washed with 2 CV of 3 M Na-acetate followed by 2 CV of high-salt buffer and finally equilibrated with 10 CV of low-salt buffer. Flow-through was collected and elution was performed stepwise with 0.2, 0.5 and 1 M NaCl.

Pichia culture medium was used for substrate specificity analyses. The fraction eluted with 0.2 M NaCl from the SP Sepharose column and containing CD2-oxidizing activity (10 μ l) was used for the determination of kinetics parameters on CDs with a degree of polymerization from 2 to 6 (results are reported in Data S2). The half-life of the enzyme was calculated as previously reported (Mauris *et al.*, 2010).

Analysis of native and oxidized oligosaccharides by HPAEC-PAD

We conducted HPAEC using an ICS3000 system (Dionex Thermo Fisher, https://www.thermofisher.com) set-up with a pulsed amperometric detector (PAD) using a gold electrode with wave-form A, according to the manufacturer's instructions. The sample

(10 μ l) was injected on a CarboPac PA1 2 \times 250 mm analytical column with a CarboPac PA1 2 \times 50 mm guard column (Dionex Thermo Fisher) kept at 35°C. Separation of oligosaccharides was obtained at a flow rate of 1 ml min⁻¹ with initial conditions set to 0.05 M KOH (100% eluent A), and applying a 20-min linear gradient to 10% B (1 M K-acetate in 0.05 M KOH) and then to 50% B in 2 min, followed by a 5-min linear gradient to 100% B; 100% B was kept for 3 min before returning to 100% A. Column reconditioning was achieved by running the initial conditions for 10 min.

Oxidation and purification of cellodextrins

Cellodextrins CD2–CD6 were purchased from ELICITYL S.A. (<https://www.elicity-oligotech.com/>). Cellodextrin purity was indicated in the datasheet provided by the manufacturer: CD2 99.3%, CD3 96.1% (with 1.2% CD2 and 1.5% CD4), CD4 97.5% (with 2.3% CD3), CD5 >90% (composition not indicated), CD6 >85% (85.8% CD6, 14.2% CD5).

CD3 or CD4 (1 mg) were dissolved in 50 mM TRIS-HCl, pH 6.8, at a final concentration of 0.8 mM. The reaction mixture (500 μ l, final volume) containing 10 μ l of SP Sepharose-purified CELLOX was incubated at 30°C for 30 h. After incubation, a small aliquot was analyzed by HPAEC-PAD in order to assess the oxidation (see below). The sample was incubated at 80°C for 15 min in order to inactivate the enzyme.

Purification of oxidized CDs was performed by HPAEC on a preparative CarboPac PA1 22 mm \times 250 mm column (Dionex Thermo Fisher) with a CarboPac PA1 9 \times 50 mm guard column kept at 30°C. Compared with the analytical method described above, the gradient profile was adjusted to meet the changed column dimensions. The sample volume of the injection loop was 500 μ l and each injection contained approximately 1 mg of each CD. The flow rate was 5 ml min⁻¹ and eluents A (0.05 M KOH) and B (1 M K-acetate in 0.05 M KOH) were applied as follows after injection: a 25-min linear gradient to 15% B and then 50% of B in 2 min, followed by a 8-min linear gradient to 100% B. 100% B was kept for 5 min before returning to 100% A and equilibrating for 15 min. Fractionation of individual cello-oligosaccharides was done without PAD detection and the oligosaccharide content of each fraction was analyzed by Dubois *et al.* (1956), checked by HPAEC-PAD using a CarboPac PA1 analytical column and mass spectrometric analysis (see above). The fraction containing oxidized CD3 was collected at 33 min at a K-Acetate concentration of 150 mM (15% B); the oxidized CD4 fraction was instead collected at 34.5 min at a K-acetate concentration of 450 mM (45% B). Fractions containing pure oxidized CDs were desalted by using GlycoProfile Glycan Clean-up Cartridges (Sigma), according to the manufacturer's instructions. Filters were incubated for 3 h with 10% acetic acid, then washed with 1 ml of acetonitrile; the carbohydrate-containing samples were loaded and left to dry for 15 min. After washing with 8 ml of acetonitrile, oligosaccharides were eluted with 2 ml of water. The eluates were lyophilized and re-dissolved in water.

Mass spectrometric analysis of oxidized cellodextrins

Electrospray ionization mass spectrometry (ESI-MS) analyses of oxidized CD3 were performed on a LTQ-Orbitrap mass spectrometer (Thermo Fisher Scientific) using positive electrospray as the ionization process. The purified oxidized CD3 (10 μ l of the purified fraction with a concentration of 354 μ g ml⁻¹) was diluted in 250 μ l of methanol:water:formic acid solvent [50:49:1 (v:v:v)] (Vuong *et al.*, 2013). The sample was introduced by direct infusion into the ESI source at a flow rate of 5 μ l min⁻¹ via a syringe pump. The MS analyses were carried out using a needle voltage of

4.5 kV and a heated capillary temperature of 300°C. Spectra acquired in the LTQ using an AGC target of 5×10^4 three microscans were recorded at a normal resolution and the maximum injection time was 200 ms. We performed MS² analyses for structural confirmation. The various parameters (collision energy, q_z activation value and activation time) were adjusted in order to optimize the signal and obtain maximal structural information from the ion of interest. In the positive ionization mode, the MS² on modified OGs only produced glycosidic bond cleavage fragments, generating B- and Y-ions, according to the nomenclature proposed by Domon and Costello (1988). The fragment ion pattern was in agreement with that obtained by Vuong *et al.* (2013).

Bioinformatic analyses

Meta-analysis of publicly available microarray data was performed using Genevestigator (Hruz *et al.*, 2008). The 3D model of CELLOX (Figure S4) was obtained with the SWISS-MODEL software (<https://swissmodel.expasy.org>) (Biasini *et al.*, 2014) using the amino acid sequence of the mature protein (i.e. without the predicted signal peptide) and the crystal structure of the monoglucan oxidase (AtBBE15; PDB ID 4ug8) as a template. The images of structural features and electrostatic potential surface were obtained using CCP4 mg (<http://www.ccp4.ac.uk/MG/references.html>) (McNicholas *et al.*, 2011). The modeled structure was compared with the 3D structure of AtBBE15 to analyze the interaction between OGOX and its cofactor FAD, using Chimera (<http://www.rbvi.ucsf.edu/chimera>) (Pettersen *et al.*, 2004). Signal peptide predictions were carried out using the Signal IP 4.1 Server (<http://www.cbs.dtu.dk/services/SignalIP/>). Amino acid identity analysis between CELLOX and the other BBE-like members was carried out using the sequences of the mature proteins and the LALIGN software (http://www.ch.embnet.org/software/LALIGN_form.html). Multiple amino acid alignment was generated using Kalign (<http://msa.sbc.su.se/cgi-bin/msa.cgi>) and the Fasta_aln file output for the software Multiple Align Show (http://www.bioinformatics.org/sms/multi_align.html).

Analyses of elicitor activity of native and oxidized cellodextrins

For gene expression analysis, 10-day-old Col-0 seedlings (grown in liquid medium) were treated for 30 min with CDs with a degree of polymerization of 2 to 6 (CD2–CD6) or oxidized CD3 and CD4 (all at 25 μ g ml⁻¹), and OGs (25 μ g ml⁻¹) as a positive control. Gene expression analyses were performed on RNA extracted from plant tissues with Nucleazol Reagent (Macherey-Nagel, <https://www.mn-net.com/>) according to the manufacturer's protocol. Complementary DNA was synthesized in a 20- μ l reaction mix using ImProm.II™ Reverse Transcriptase (Promega). Real-time quantitative PCR analysis was performed using a CFX96 Real-Time System (Bio-Rad, <http://www.bio-rad.com/>) and the reaction was carried out in a mix containing 1 \times Go Taq qPCR Master Mix (Promega) and 0.5 μ M of each primer. The expression levels of each gene, relative to UBQ5, were determined using a modification of the Pfaffl method (Pfaffl, 2001) as previously described (Ferrari *et al.*, 2006).

For analysis of MAPK3/6 phosphorylation, seedlings were treated for 5 and 15 min with 30 μ M CDs (CD2 9.96 μ g ml⁻¹, CD3 15 μ g ml⁻¹, CD4 19.5 μ g ml⁻¹, CD5 25.5 μ g ml⁻¹, CD6 30 μ g ml⁻¹) and OGs (40 μ g ml⁻¹). Protein extraction and immunoblot assays were performed as previously described (Galletti *et al.*, 2011; Savatin *et al.*, 2014a). For ROS measurements, leaf disks of 4-week-old Col-0 plants were vacuum infiltrated with CDs or OGs (all at

350 $\mu\text{g ml}^{-1}$) and H_2O_2 detection was performed by a luminol-based assay as previously described (Gigli-Bisceglia *et al.*, 2015).

Generation of transgenic plants

The At4g20860 DNA sequence from the translation initiation codon to the termination codon was amplified from *Arabidopsis* gDNA using the *Sma*I-Fw and *Sac*I-Rev primers (Table S1). The fragment was cloned using the *Sma*I and *Sac*I restriction sites of pBI121, replacing the β -glucuronidase gene sequence. The recombinant plasmid was introduced into *Agrobacterium tumefaciens* strain GV3101 by electroporation and *A. thaliana* Col-0 plants were transformed using the floral dip method. For segregation analysis, seeds were germinated on plates containing solid MS/2 medium [MS Basal Medium (2.15 g L^{-1}), 1% sucrose, 0.8% plant agar, pH 5.5], supplemented with kanamycin (20 $\mu\text{g ml}^{-1}$) as a selective agent and grown at 22°C and 70% relative humidity under a 16-h light/8-h dark cycle. From 18 independent transformed lines, five T₃ homozygous lines (CELLOX-OE #2.6, #4.4, #7.2, #8.5 and #9.7) carrying a single insertion of the transgene cassette were selected for further analysis.

For measurements of the oxidizing activity, total proteins were extracted from 2 g of fresh leaf material of CELLOX-OE plants, using 8 ml of extraction buffer (20 mM Na-acetate pH 5.0, 0.8 M NaCl). Activity was determined using 0.2 M CD3, a 60-min incubation time and the xylenol orange assay.

Botrytis cinerea infection assay and growth

Botrytis cinerea was grown on 20 g L^{-1} malt extract, 10 g L^{-1} proteose peptone n.3 (Difco, <https://www.fishersci.it/it/home.html>), and 15 g L^{-1} agar for 7–10 days at 24°C with a 12-h photoperiod before the collection of spores. Rosette leaves from 4-week-old soil-grown *Arabidopsis* plants were placed in Petri dishes containing 0.8% agar, with the petiole embedded in the medium. Inoculation was performed by placing 5 μl of a suspension of 5×10^5 conidiospores ml^{-1} in 24 g L^{-1} potato dextrose broth (PDB; Difco) on each side of the middle vein. The plates were incubated at 22°C with a 12-h photoperiod. High humidity was maintained by covering the plates with a clear plastic lid. Under these experimental conditions, most inoculations resulted in rapidly expanding water-soaked lesions of comparable diameter. Lesion size was determined by measuring the diameter or, in the case of oval lesions, the major axis of the necrotic area by using ImageJ software.

In vitro assay of *B. cinerea* growth assay was performed in a 24-well MULTIWELL plate (Falcon, Becton Dickinson Labware, <https://www.bd.com/>) containing 0.5 ml of a modified pectic zymogram (PZ) medium [20 mM $(\text{NH}_4)_2\text{SO}_4$, 2.5 mM KH_2PO_4 and 0.6 mM MgSO_4]. For growth in the presence of CD3, PZ was supplied with 0.15% (w/v) CD3, purified oxidized CD3 (prepared as described above) or both; the pH was adjusted to 4.7 in all cases. Each well was inoculated with 7×10^4 conidiospores. Six replicates were prepared for each sample. Plates were incubated at 22°C for 96 h at 75 r.p.m. For fungal biomass determination, two pools of three replicates were obtained, dried and weighed. Standard deviation was calculated from the mean of the two different pools.

Analysis of CD3 and oxidized CD3 in Col-0 and CELLOX-OE plants by HPAEC-PAD

Four-week-old Col-0 and CELLOX-OE leaves were infiltrated with H_2O (control) and CD3 (500 $\text{ng } \mu\text{l}^{-1}$) using a 1-ml syringe without a needle (approximately 100 μl per leaf). Thirty minutes after infiltration, the infiltrated tissues of a pool of 10 leaves, cut into strips, for each genotype and treatment were collected and vacuum

infiltrated for 10 min with intercellular washing fluid (IWF) extraction buffer (50 mM KPO_4 pH 8.0, 0.5 M KCl). The IWFs were recovered by centrifuging for 10 min at 5000 *g*. About 100 μl of IWF was collected for each sample and analyzed by HPAEC-PAD as described above.

ACCESSION NUMBERS

At4g20860

ACKNOWLEDGEMENTS

This work was supported by the Institute Pasteur Fondazione Cenci Bolognetti and by Sapienza University of Rome. We thank Professor Antonio Molinaro (Federico II University of Naples, Italy) for the kind gift of xyloglucan. We thank Dr Ilaria Verrascina for contributing to the generation of transgenic plants.

CONFLICT OF INTEREST

The authors declare no conflict of interest.

SUPPORTING INFORMATION

Additional Supporting Information may be found in the online version of this article.

Figure S1. Homology tree of the berberine bridge enzyme-like family protein members.

Figure S2. Heatmap of the expression of the 27 members of berberine bridge enzyme-like family upon treatment with elicitors or pathogens.

Figure S3. Substrate specificity of cellodextrin oxidase.

Figure S4. Enrichment of recombinant cellodextrin oxidase secreted by the transformed *Pichia pastoris* through a two-step ion exchange chromatography.

Figure S5. High performance anion exchange chromatography with pulsed amperometric detection and MS analysis of native and oxidized cellotriose and cellotetraose.

Figure S6. Characteristics of cellodextrin oxidase and its gene.

Figure S7. Active site of cellodextrin oxidase.

Table S1. Primers used in this work.

Data S1. Proteins identified by LC-MS/MS analysis of the fractions obtained by OG-machine leaf protein extract after elution from sulfopropyl Sepharose cation exchange column.

Data S2. Calculation of K_m , V_{max} and thermostability of cellodextrin oxidase expressed in *Pichia pastoris*.

REFERENCES

- Aziz, A., Gauthier, A., Bézier, A., Poinssot, B., Joubert, J.M., Pugin, A., Heyraud, A. and Baillieu, F. (2007) Elicitor and resistance-inducing activities of beta-1,4 cellodextrins in grapevine, comparison with beta-1,3 glucans and alpha-1,4 oligogalacturonides. *J. Exp. Bot.* **58**, 1463–1472.
- Bacete, L., Melida, H., Miedes, E. and Molina, A. (2018) Plant cell wall-mediated immunity: cell wall changes trigger disease resistance responses. *Plant J.* **93**, 614–636.
- Becker, D., Binda, C., Ceccarelli, E., Chaiyen, P., Costa Filho, A.J., Daniel, B., Dully, C., Edmondson, D., Fitzpatrick, P. and Gadda, G. (2012) *Handbook of Flavoproteins: Oxidases, Dehydrogenases and Related Systems*, vol. 1. Berlin: De Gruyter.
- Benedetti, M., Leggio, C., Federici, L., De Lorenzo, G., Pavel, N.V. and Cervone, F. (2011) Structural resolution of the complex between a fungal polygalacturonase and a plant polygalacturonase-inhibiting protein by small-angle X-ray scattering. *Plant Physiol.* **157**, 599–607.
- Benedetti, M., Andreani, F., Leggio, C., Galantini, L., Di Matteo, A., Pavel, N.V., De Lorenzo, G., Cervone, F., Federici, L. and Sicilia, F. (2013) A single amino-acid substitution allows endo-polygalacturonase of *Fusarium*

- verticillioides* to acquire recognition by PGIP2 from *Phaseolus vulgaris*. *PLoS ONE* **8**, e80610.
- Benedetti, M., Pontiggia, D., Raggi, S., Cheng, Z., Scaloni, F., Ferrari, S., Ausubel, F.M., Cervone, F. and De Lorenzo, G. (2015) Plant immunity triggered by engineered in vivo release of oligogalacturonides, damage-associated molecular patterns. *Proc. Natl Acad. Sci. USA* **112**, 5533–5538.
- Benedetti, M., Verrascina, I., Pontiggia, D., Locci, F., Mattei, B., De Lorenzo, G. and Cervone, F. (2018) Four Arabidopsis berberine bridge enzyme-like proteins are specific oxidases that inactivate the elicitor-active oligogalacturonides. *Plant J.* **94**, 260–273.
- Biasini, M., Bienert, S., Waterhouse, A. et al. (2014) SWISS-MODEL: modelling protein tertiary and quaternary structure using evolutionary information. *Nucleic Acids Res.* **42**, W252–W258.
- Boutrot, F. and Zipfel, C. (2017) Function, discovery, and exploitation of plant pattern recognition receptors for broad-spectrum disease resistance. *Annu. Rev. Phytopathol.* **55**, 257–286.
- Carter, C.J. and Thornburg, R.W. (2004) Tobacco nectarin V is a flavin-containing berberine bridge enzyme-like protein with glucose oxidase activity. *Plant Physiol.* **134**, 460–469.
- Casoli, M., Federici, L., Spinelli, F., Di Matteo, A., Vella, N., Scaloni, F., Fernandez-Recio, J., Cervone, F. and De Lorenzo, G. (2009) Integration of evolutionary and desolvation energy analysis identifies functional sites in a plant immunity protein. *Proc. Natl Acad. Sci. USA*, **106**, 7666–7671.
- Cervone, F., De Lorenzo, G., Degrà, L. and Salvi, G. (1987) Elicitation of necrosis in *Vigna unguiculata* Walp. by homogeneous *Aspergillus niger* endo-polygalacturonase and by α -D-galacturonate oligomers. *Plant Physiol.* **85**, 626–630.
- Cervone, F., Ausubel, F.M. and De Lorenzo, G. (2015) Enhancing immunity by engineering DAMPs. *Oncotarget*, **6**, 28523–28524.
- Claverie, J., Balacey, S., Lemaitre-Guillier, C. et al. (2018) The cell wall-derived xyloglucan is a new DAMP triggering plant immunity in *Vitis vinifera* and *Arabidopsis thaliana*. *Front. Plant Sci.* **9**, 1725.
- Cosgrove, D.J. (2017) Microbial expansins. *Annu. Rev. Microbiol.* **71**, 479–497.
- Custers, J.H., Harrison, S.J., Sela-Buurlage, M.B. et al. (2004) Isolation and characterisation of a class of carbohydrate oxidases from higher plants, with a role in active defence. *Plant J.* **39**, 147–160.
- Daniel, B., Pavkov-Keller, T., Steiner, B. et al. (2015) Oxidation of monolignols by members of the berberine-bridge enzyme family suggests a role in plant cell wall metabolism. *J. Biol. Chem.* **290**, 18770–18781.
- Daniel, B., Wallner, S., Steiner, B., Oberdorfer, G., Kumar, P., van der Graaff, E., Roitsch, T., Sensen, C.W., Gruber, K. and Macheroux, P. (2016) Structure of a berberine bridge enzyme-like enzyme with an active site specific to the plant family brassicaceae. *PLoS ONE*, **11**, e0156892.
- Daniel, B., Konrad, B., Toplak, M., Lahham, M., Messenlehner, J., Winkler, A. and Macheroux, P. (2017) The family of berberine bridge enzyme-like enzymes: a treasure-trove of oxidative reactions. *Arch. Biochem. Biophys.* **632**, 88–103.
- Darvill, A., Bergmann, C., Cervone, F., De Lorenzo, G., Ham, K.S., Spiro, M.D., York, W.S. and Albersheim, P. (1994) Oligosaccharins involved in plant growth and host-pathogen interactions. *Biochem. Soc. Symp.* **60**, 89–94.
- De Lorenzo, G., Ferrari, S., Cervone, F. and Okun, E. (2018a) Extracellular DAMPs in plants and mammals: immunity, tissue damage and repair. *Trends Immunol.* **39**, 937–950.
- De Lorenzo, G., Ferrari, S., Giovannoni, M., Mattei, B. and Cervone, F. (2018b) Cell wall traits that influence plant development, immunity and bioconversion. *Plant J.* **97**, 134–147.
- Denoux, C., Galletti, R., Mammarella, N., Gopalan, S., Werck, D., De Lorenzo, G., Ferrari, S., Ausubel, F.M. and Dewdney, J. (2008) Activation of defense response pathways by OGs and Flg22 elicitors in Arabidopsis seedlings. *Mol. Plant*, **1**, 423–445.
- Domon, B. and Costello, C.E. (1988) A systematic nomenclature for carbohydrate fragmentations in FAB-MS/MS spectra of glycoconjugates. *Glycoconjugate J.* **5**, 397–409.
- Dubois, M., Gilles, K.A., Hamilton, J.K., Rebers, P.A. and Smith, F. (1956) Colorimetric methods for determination of sugars and related substances. *Anal. Chem.* **28**, 350–358.
- Engelsdorf, T., Gigli-Bisceglia, N., Veerabagu, M., McKenna, J.F., Vaahtera, L., Augstein, F., Van der Does, D., Zipfel, C. and Hamann, T. (2018) The plant cell wall integrity maintenance and immune signaling systems cooperate to control stress responses in *Arabidopsis thaliana*. *Sci. Signal.* **11**, eaao3070.
- Ferrari, S., Galletti, R., Vairo, D., Cervone, F. and De Lorenzo, G. (2006) Antisense expression of the *Arabidopsis thaliana* AtPGIP1 gene reduces polygalacturonase-inhibiting protein accumulation and enhances susceptibility to *Botrytis cinerea*. *Mol. Plant-Microbe Interact.* **19**, 931–936.
- Ferrari, S., Savatin, D.V., Sicilia, F., Gramegna, G., Cervone, F. and Lorenzo, G.D. (2013) Oligogalacturonides: plant damage-associated molecular patterns and regulators of growth and development. *Front. Plant Sci.* **4**, 49.
- Franck, C.M., Westermann, J. and Boisson-Dernier, A. (2018) Plant malectin-like receptor kinases: from cell wall integrity to immunity and beyond. *Annu. Rev. Plant Biol.* **69**, 301–328.
- Galletti, R., Ferrari, S. and De Lorenzo, G. (2011) Arabidopsis MPK3 and MPK6 play different roles in basal and oligogalacturonide- or flagellin-induced resistance against *Botrytis cinerea*. *Plant Physiol.* **157**, 804–814.
- Gay, C., Collins, J. and Gebicki, J.M. (1999) Hydroperoxide assay with the ferric-xylenol orange complex. *Anal. Biochem.* **273**, 149–155.
- Gigli-Bisceglia, N., Gravino, M. and Savatin, D.V. (2015) Luminol-based assay for detection of immunity elicitor-induced hydrogen peroxide production in *Arabidopsis thaliana* leaves. *Bio-protocol*, **5**, e1685.
- Gravino, M., Savatin, D.V., Maccone, A. and De Lorenzo, G. (2015) Ethylene production in *Botrytis cinerea*- and oligogalacturonide-induced immunity requires calcium-dependent protein kinases. *Plant J.* **84**, 1073–1086.
- Gust, A.A., Pruitt, R. and Nürnberg, T. (2017) Sensing danger: key to activating plant immunity. *Trends Plant Sci.* **22**, 779–791.
- Hruz, T., Laule, O., Szabo, G., Wessendorp, F., Bleuler, S., Oertle, L., Widmayer, P., Gruissem, W. and Zimmermann, P. (2008) Genevestigator v3: a reference expression database for the meta-analysis of transcriptomes. *Adv. Bioinform.* **2008**, 420747.
- Huang, C.H., Lai, W.L., Lee, M.H., Chen, C.J., Vasella, A., Tsai, Y.C. and Liaw, S.H. (2005) Crystal structure of glucooligosaccharide oxidase from *Acremonium strictum*: a novel flavinylation of 6-S-cysteinylnyl, 8 α -N1-histidyl FAD. *J. Biol. Chem.* **280**, 38831–38838.
- Huot, B., Yao, J., Montgomery, B.L. and He, S.Y. (2014) Growth-defense tradeoffs in plants: a balancing act to optimize fitness. *Mol. Plant*, **7**, 1267–1287.
- Johnson, J.M., Thurich, J., Petutschnig, E.K. et al. (2018) A Poly(A) ribonuclease controls the cellotriose-based interaction between *Piriformospora indica* and its host *Arabidopsis*. *Plant Physiol.* **176**, 2496–2514.
- Lampugnani, E.R., Khan, G.A., Somssich, M. and Persson, S. (2018) Building a plant cell wall at a glance. *J. Cell Sci.* **131**, jcs207373.
- Maisuria, V.B., Patel, V.A. and Nerurkar, A.S. (2010) Biochemical and thermal stabilization parameters of polygalacturonase from *Erwinia carotovora* subsp. *carotovora* BR1. *J. Microbiol. Biotechnol.* **20**, 1077–1085.
- Malinovsky, F.G., Fangel, J.U. and Willats, W.G. (2014) The role of the cell wall in plant immunity. *Front. Plant Sci.* **5**, 178.
- Mattei, B., Spinelli, F., Pontiggia, D. and De Lorenzo, G. (2016) Comprehensive analysis of the membrane phosphoproteome regulated by oligogalacturonides in *Arabidopsis thaliana*. *Front. Plant Sci.* **7**, 1107.
- McNicholas, S., Potterton, E., Wilson, K.S. and Noble, M.E. (2011) Presenting your structures: the CCP4 molecular-graphics software. *Acta Crystallogr. D Biol. Crystallogr.* **67**, 386–394.
- Meyer, A.J., Riemer, J. and Rouhier, N. (2019) Oxidative protein folding: state-of-the-art and current avenues of research in plants. *New Phytol.* **221**, 1230–1246.
- Oelmüller, R. (2018) Sensing environmental and developmental signals via cellooligosaccharides. *J. Plant Physiol.* **229**, 1–6.
- Pettersen, E.F., Goddard, T.D., Huang, C.C., Couch, G.S., Greenblatt, D.M., Meng, E.C. and Ferrin, T.E. (2004) UCSF Chimera—a visualization system for exploratory research and analysis. *J. Comput. Chem.* **25**, 1605–1612.
- Pfaffl, M.W. (2001) A new mathematical model for relative quantification in real-time RT-PCR. *Nucleic Acids Res.* **29**, e45.
- Rajniak, J., Barco, B., Clay, N.K. and Sattely, E.S. (2015) A new cyanogenic metabolite in *Arabidopsis* required for inducible pathogen defence. *Nature*, **525**, 376–379.
- Roux, M., Schwessinger, B., Albrecht, C., Chinchilla, D., Jones, A., Holton, N., Malinovsky, F.G., Tor, M., de Vries, S. and Zipfel, C. (2011) The *Arabidopsis* leucine-rich repeat receptor-like kinases BAK1/SERK3 and BKK1/SERK4 are required for innate immunity to hemibiotrophic and biotrophic pathogens. *Plant Cell*, **23**, 2440–2455.

- Savatin, D.V., Gigli-Bisceglia, N., Marti, L., Fabbri, C., Cervone, F. and De Lorenzo, G.** (2014a) The Arabidopsis NUCLEUS- AND PHRAGMOPLAST-LOCALIZED KINASE1-related protein kinases are required for elicitor-induced oxidative burst and immunity. *Plant Physiol.* **165**, 1188–1202.
- Savatin, D.V., Gramegna, G., Modesti, V. and Cervone, F.** (2014b) Wounding in the plant tissue: the defense of a dangerous passage. *Front. Plant Sci.* **5**, 470.
- Souza, C.A., Li, S., Lin, A.Z., Boutrot, F., Grossmann, G., Zipfel, C. and Somerville, S.C.** (2017) Cellulose-derived oligomers act as damage-associated molecular patterns and trigger defense-like responses. *Plant Physiol.* **173**, 2383–2398.
- Toplak, M., Wiedemann, G., Ulicevic, J., Daniel, B., Hoernstein, S.N.W., Kothe, J., Niederhauser, J., Reski, R., Winkler, A. and Macheroux, P.** (2018) The single berberine bridge enzyme homolog of *Physcomitrella patens* is a cellobiose oxidase. *FEBS J.* **285**, 1923–1943.
- Tucker, M.R., Lou, H., Aubert, M.K., Wilkinson, L.G., Little, A., Houston, K., Pinto, S.C. and Shirley, N.J.** (2018) Exploring the role of cell wall-related genes and polysaccharides during plant development. *Plants (Basel)*, **7**, E42.
- Vuong, T.V., Vesterinen, A.H., Foumani, M., Juvonen, M., Seppala, J., Tenkanen, M. and Master, E.R.** (2013) Xylo- and cello-oligosaccharide oxidation by gluco-oligosaccharide oxidase from *Sarocladium strictum* and variants with reduced substrate inhibition. *Biotechnol. Biofuels*, **6**, 148.
- Winkler, A., Hartner, F., Kutchan, T.M., Glieder, A. and Macheroux, P.** (2006) Biochemical evidence that berberine bridge enzyme belongs to a novel family of flavoproteins containing a bi-covalently attached FAD cofactor. *J. Biol. Chem.* **281**, 21276–21285.
- Wolf, S.** (2017) Plant cell wall signalling and receptor-like kinases. *Biochem. J.* **474**, 471–492.
- Yi, M.C. and Khosla, C.** (2016) Thiol-disulfide exchange reactions in the mammalian extracellular environment. *Annu. Rev. Chem. Biomol. Eng.* **7**, 197–222.
- Zafred, D., Steiner, B., Teufelberger, A.R., Hromic, A., Karplus, P.A., Schofield, C.J., Wallner, S. and Macheroux, P.** (2015) Rationally engineered flavin-dependent oxidase reveals steric control of dioxygen reduction. *FEBS J.* **282**, 3060–3074.